PAPER

The aromatic character of thienopyrrole-modified 20π-electron porphyrinoids†

Rashid R. Valiev,*[ab] Heike Fliegl*[c] and Dage Sundholm*[d]

Magnetically induced current densities and current pathways have been calculated for six tautomers of substituted and nonsubstituted core-modified porphyrinoids with one of the pyrrole rings replaced by a thienopyrrole moiety. The calculations show that the aromatic properties of the porpyrinoid macrocycle are strongly influenced by the ethyl-formate substituent at the pyrrole ring of the thienopyrrole moiety, whereas the alkyl substituents at the β positions of the ordinary pyrrole rings have a much smaller effect on the ring-current strength. The ethyl-formate substitution decreases the strength of the paratropic ring current of the macrocycle rendering the energetically lowest tautomer nonaromatic. The substituted tautomers with both porphyrinoid hydrogens inside the macroring are antiaromatic according to the ring current criterion, whereas the three tautomers with one hydrogen at the outer nitrogen of the thienopyrrole moiety are nonaromatic. Current calculations on the nonsubstituted core-modified porphyrinoids show that they are all antiaromatic. The antiaromatic thienopyrrole-modified porphyrinoids are dominated by paratropic ring currents inside the macroring and a weaker diatropic current along the periphery of the macroring. The nonaromatic porphyrinoid tautomers sustain significant ring currents around the thienopyrrole moiety, whereas the other pyrrole rings are practically nonaromatic.

1 Introduction

Porphyrinoid based materials are employed in molecular electronics, non-linear optics and biomedical applications. Porphyrins also play important roles in many biochemical processes. The usability of porphyrins and porphyrinoids in technological applications depends on molecular properties associated with the aromatic conjugation of the porphyrin macrocycle. Thus, to design porphyrinoids with specific properties, it is necessary to elucidate the aromatic character of the macrocycle. The aromatic properties of porphyrinoids with complex multiring structures have therefore been investigated in the past few years computationally and experimentally by a number of research groups.[1–16]

The development of specialized computational methods has made computational studies a valuable tool for comprehensive and quantitative studies of the aromatic character of molecules.[10,11,17–21] The gauge including magnetically induced current method (GIMIC)[17,22] has proven to be a very reliable method to quantifying molecular aromaticity and to determining the pathways of the current flow in molecules when they are exposed to an external magnetic field. The degree of aromaticity is very hard to assess experimentally, whereas computationally it can be obtained by calculating the current pathways and the current susceptibilities of individual chemical bonds. The current susceptibility passing through a selected chemical bond, which is also called the current strength, can be used as an aromaticity index for quantifying the aromatic character of molecules. The sign and magnitude of the current strength indicate whether a molecular ring is aromatic, antiaromatic or nonaromatic. Aromatic rings sustain a diatropic ring current, which is a ring current flowing in the classical direction inducing a magnetic field in the direction opposite to the applied external one. For antiaromatic molecules, the induced paratropic ring current flows in the non-classical direction. Non-aromatic molecules sustain diatropic and paratropic currents of the same size leading to a vanishing net ring current.[23]

The GIMIC method has been employed in studies of the magnetically induced current pathways and ring-current strengths of porphyrins, chlorins, bacteriochlorins, and thieno-bridged porphyrins.[17,19,20] The GIMIC studies unambiguously show that neither the 18π [18]annulene picture,[24–28] where the inner NH groups act as inert bridges, nor the more recently proposed

[a] *Tomsk State University, Lenina 36, Tomsk, Russian Federation.*
  E-mail: valievrashid@mail.ru
[b] *Tomsk Polytechnic University, 43a Lenin Avenue, Building 2, Tomsk 634050, Russian Federation*
[c] *Centre for Theoretical and Computational Chemistry (CTCC), Department of Chemistry, University of Oslo, P.O. Box 1033 Blindern, 0315 Oslo, Norway. E-mail: heike.fliegl@kjemi.uio.no*
[d] *Department of Chemistry, University of Helsinki, P.O. Box 55 (A.I. Virtanens plats 1), FIN-00014, Finland. E-mail: dage.sundholm@helsinki.fi*

† Electronic supplementary information (ESI) available: The optimized Cartesian coordinates, the calculated vibrational frequencies and the calculated NMR shielding constants of the six tautomers are given. The same data for the nonsubstituted porphyrinoids are also reported. See DOI: 10.1039/c4cp00883a

18π [16]annulene inner cross route[29,30] is the correct description of the aromatic pathway of porphyrins.[31–33] The GIMIC calculations[19,20] also indicated that the current pathways of porphyrins and porphyrinoids cannot be reliably obtained by using nucleus independent chemical shift (NICS) calculations.[34] The GIMIC study of the current pathways of thieno-bridged porphyrins showed that the combination of NICS calculations and calculations of the anisotropy of the magnetically induced current-density (ACID)[35,36] do not necessarily lead to a correct understanding of the aromatic character of molecules with a complex molecular structure consisting of fused conjugated rings. The GIMIC calculations on tetraoxa-isophlorin and dioxo-dithia-isophlorin with formally $4N$ π electrons showed that the isophlorins are strongly antiaromatic sustaining large paratropic ring currents around the porphyrinoid macroring.[21]

Recently, Chang *et al.* reported the synthesis and characterization of a core-modified porphyrinoid that consists of a porphyrin with one of the pyrrole rings replaced by a thienopyrrole moiety.[37] In the experimental characterization, they found that the optical and redox properties of this formally 20π electron system remarkably differ from those of conventional porphyrins with formally 18π electrons. Proton nuclear magnetic resonance (NMR) spectroscopy studies as well as combined ACID and NICS calculations suggested that the thienopyrrole-modified porphyrinoid is nonaromatic, which is indeed somewhat surprising since porphyrinoids with formally 20π electrons have recently been found to be antiaromatic rather than nonaromatic.[21]

Since it has been shown that GIMIC calculations yield reliable information about the aromatic character of porphyrinoids, the aim of the present work is to elucidate the aromatic character of the different tautomers of the thienopyrrole-modified porphyrinoid. We also investigate how the ethyl and methyl substituents at the β positions of the pyrrole rings and the ethyl-formate substituent of the thienopyrrole ring affect the current strength of the porphyrinoid macrocycle.

In Section 2, we describe the computational methods employed. The optimized molecular structures of the tautomers are discussed in Section 3 and their relative energies in Section 4. The calculated ^{1}H NMR chemical shifts are compared to experimental data in Section 5. The current strengths calculated for the six tautomers are discussed in Section 6 and the main conclusions are presented in Section 7.

2 Computational details

The molecular structures of the six tautomers of the thienopyrrole-modified porphyrinoid molecule were optimized at the density functional theory (DFT) level using the B3LYP functional[38,39] and a triple-ζ quality basis set augmented with polarization functions (def2-TZVP);[40] def2 is omitted in the discussion. The optimized molecular structures are minima on the potential energy surface since in the calculations of the vibrational spectra no imaginary frequencies were obtained. Nuclear magnetic shieldings were calculated at the same level of theory.[41,42] In a recent study, nuclear magnetic shieldings calculated at the DFT level using

different functionals were compared to coupled-cluster data showing that the B3LYP functional provides reasonable accurate NMR shielding constants.[43] The solvent effects on the relative energies were considered using conductor-like screening model (COSMO) calculations with a dielectric constant of 4.7113 simulating CDCl$_3$.[44] The molecular structure optimizations and the calculation of the nuclear magnetic shieldings were performed using TURBOMOLE version 6.5.[45]
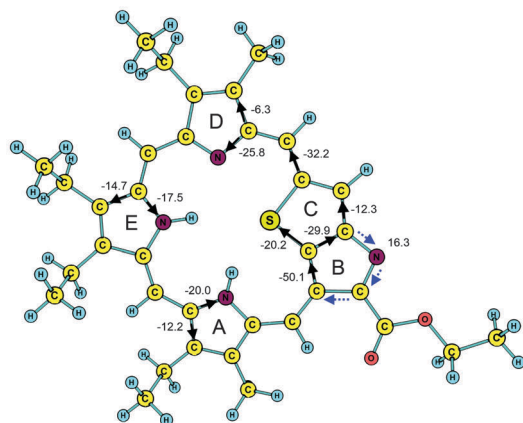
The magnetically induced current densities were obtained by the GIMIC method.[17,22] GIMIC is an independent program that uses the magnetically perturbed one-electron density matrices of nuclear magnetic shielding calculations, the one-electron density matrix, and basis-set information as input data.[17,22] Gauge-including atomic orbitals (GIAO) have been employed in the NMR shielding and GIMIC calculations for obtaining gauge origin independent current densities.[46–49] The ring-current susceptibility (in nA T^{-1}) is denoted ring-current strength in the rest of the article. The current strengths and current pathways were obtained by numerical integration of the current density passing through cut planes perpendicularly to selected bonds of the molecule. The calculated current strength is a reliable measure of the degree of molecular aromaticity.[18] The current strength can be used as an aromaticity index when using a ring-current strength of 11.8 nA T^{-1} for benzene calculated at the B3LYP/TZVP level as reference value and considering that nonaromatic molecules do not sustain any net ring current. The current density plots have been generated using JMOL.[50] The pictures of current pathways have been aquired using GIMP.[51]
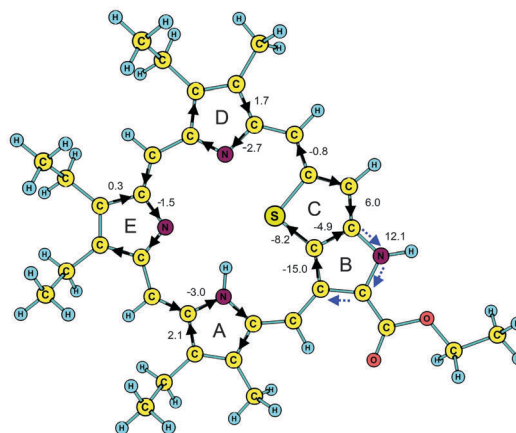
3 Molecular structures

Fig. 1 and 2 show the equilibrium structures of the studied tautomers of the substituted thienopyrrole-modified porphyrinoid. The structures of the tautomers of the nonsubstituted thienopyrrole-modified porphyrinoid are shown in the ESI.† The Cartesian coordinates of the studied molecules are given as ESI.† The optimized molecular structures agree well with X-ray data.[37]
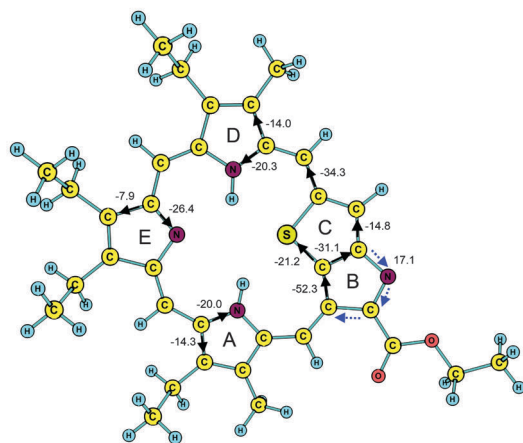
4 Relative energies

The calculated relative energies with respect to the lowest tautomer (2–4) are given in Fig. 1 and 2 and gathered in Table 1. Since the relative energy of tautomer 2–4 is 6.0 kcal mol^{-1} below the second lowest tautomer (1–2), a Boltzmann distribution suggests that tautomer 2–4 completely dominates in the thermal mixture at room temperature. The experimental ^{1}H NMR spectrum of the synthesized thienopyrrole-modified porphyrinoid reported in the ESI† of ref. 37 suggests that only one tautomer is obtained in the synthesis. The energy differences between the tautomers are though rather small as the energy of the energetically highest tautomer (2–3) is 12.8 kcal mol^{-1} above tautomer 2–4. The second lowest tautomer is 1–2, which is antiaromatic sustaining a strong paratropic ring current of -32.2 nA T^{-1} around the porphyrinoid macrocycle. The tautomers with an outer pyrrole hydrogen can form a hydrogen bond
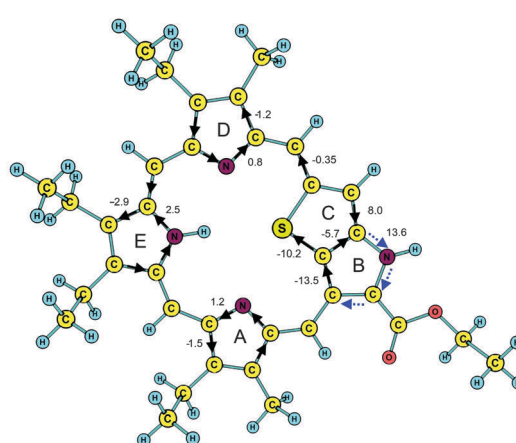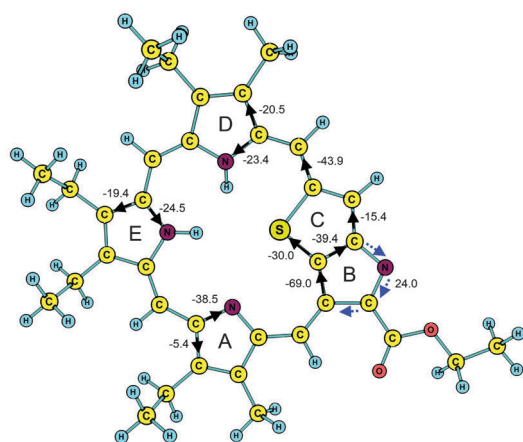
This journal is © the Owner Societies 2014

Phys. Chem. Chem. Phys., 2014, **16**, 11010–11016 | **11011**

(a) Tautomer 1-2 (6.0 kcal/mol)

(b) Tautomer 1-3 (7.4 kcal/mol)

(c) Tautomer 2-3 (12.8 kcal/mol)

Fig. 1 The molecular structures of the substituted (a) 1–2, (b) 1–3, and (c) 2–3 tautomers, where position 1 is the nitrogen in ring A. The inner nitrogens are numbered clockwise and position 4 is the nitrogen in ring B. The current strengths passing chemical bonds and relative energies are also given. The arrows indicate the current pathways. The blue arrows show the diatropic ring current around ring B.

(a) Tautomer 1-4 (9.7 kcal/mol)

(b) Tautomer 2-4 (0.0 kcal/mol)

(c) Tautomer 3-4 (6.3 kcal/mol)

Fig. 2 The molecular structures of the substituted (a) 1–4, (b) 2–4, and (c) 3–4 tautomers. The numbering of the pyrrole nitrogens is given in the caption of Fig. 1. The inner nitrogens are numbered clockwise and position 4 is the nitrogen in ring B. The current strengths passing chemical bonds and relative energies are also given. The arrows indicate the current pathways. The blue arrows show the diatropic ring current around ring B.

with the oxygen atom of the ester group. The strength of the hydrogen bond was estimated from the current strength passing back and forth across the bond.[52] The calculations yielded a

hydrogen-bond strength of 3.0 kcal mol^{-1} for tautomer 2–4, whereas for the other two tautomers with an outer pyrrole hydrogen the hydrogen bond strengths are 6.0 kcal mol^{-1} (1–4) and

11012 | Phys. Chem. Chem. Phys., 2014, 16, 11010–11016

This journal is © the Owner Societies 2014

Table 1 The relative energies (in kcal mol^{-1}) of the tautomers of the substituted and nonsubstituted thienopyrrole-modified porphyrinoids. We also report relative energies for the substituted tautomers that were obtained using COSMO to consider the solvent effects. The energy of the lowest tautomer (2–4) is the reference energy. The relative order of the substituted tautomers is also given

| Tautomer | Order | Substituted | | Nonsubstituted |
		Vacuum	COSMO	
1–2	2	6.0	5.1	2.4
1–3	4	7.4	6.9	3.8
2–3	6	12.8	10.6	7.8
1–4	5	9.7	8.9	11.4
2–4	1	0.0	0.0	0.0
3–4	3	6.3	5.5	6.8

Table 2 The ^{1}H NMR chemical shifts (in ppm) for the six tautomers of the thienopyrrole-modified porphyrinoid. The experimental data for tautomer 2–4 are given in the last column[37]

Peak^a	1–2	1–3	2–3	1–4	2–4	3–4	Exp.
H$_{AB}$	3.81	3.27	2.49	7.47	8.26	8.45	7.46
H$_{CD}$	1.46	−0.10	−1.27	6.83	6.88	6.43	6.54
H$_{DE}$	0.04	−0.80	−2.91	6.01	5.73	5.80	5.31
H$_{AE}$	−1.03	−0.70	−1.50	5.36	5.84	6.55	5.36
TH	2.99	2.37	1.60	6.55	6.67	6.56	6.62
NH$_{in}$	33.66	36.46	41.09	12.07	12.33	13.72	12.85
NH$_{in}$	33.59	36.94	37.29				
NH$_{out}$				7.92	8.24	8.32	8.83

^{a} H$_{ij}$ denotes the meso hydrogen between rings i and j. TH is the thiophene hydrogen, NH$_{in}$ and NH$_{out}$ are the inner and outer pyrrole hydrogens of the tautomers 1–4, 2–4 and 3–4. Tautomers 1–2, 1–3, and 2–3 have only inner pyrrole hydrogens.

5.0 kcal mol^{-1} (3–4). The binding energies of the hydrogen bonds estimated from the current strength passing the bond agree well with the differences in the relative energies between the substituted and nonsubstituted tautomers reported in Table 1. The relative energies in Table 1 also show that neither the antiaromatic character of the tautomers with two inner hydrogens nor the position of the pyrrole hydrogens influences the relative energies in any obvious way.

The 2–4 tautomer is also the energetically lowest one when the solvent effects are considered using COSMO. At the B3LYP/TZVP level, the solvent effects lower the relative tautomer energies by 0.5–2.2 kcal mol^{-1} (7–17%) without changing the energetic order of the tautomers. For the nonsubstituted porphyrinoids, the relative energies of the tautomers with two inner hydrogens are 3.6–5.0 kcal mol^{-1} smaller than those of the corresponding substituted ones, because of the formation of the hydrogen bond between the outer pyrrole hydrogen and the ester oxygen of the ethyl-formate group.

5 ^{1}H NMR shieldings

The calculated nuclear magnetic shieldings for all tautomers of the substituted and nonsubstituted porphyrinoids are given in the ESI.† The nuclear magnetic shieldings for the hydrogens of the tetramethylsilane (TMS) reference calculated at the same level of theory are 31.91 ppm. The calculated ^{1}H NMR chemical shifts of the four meso-protons and the thiophene hydrogen of the substituted 2–4 tautomer are 5.73, 5.84, 6.88, 8.26, and 6.67 ppm, which can be compared to the experimental ^{1}H NMR chemical shifts of 5.31, 5.36, 6.54, 6.62, and 7.46 ppm, respectively, reported by Chang *et al.* in the supporting information of their article[37] These signals in the experimental spectrum have not been assigned, whereas in the ^{1}H NMR spectrum reported in their main article Chang *et al.* assigned the peaks at 4.82, 4.97, 6.20 and 6.57 ppm to the hydrogens at the meso carbons and the peak originating from hydrogen at the thiophene ring appears at 7.16 ppm.[37] It is not evident from their article how the different ^{1}H NMR spectra have been recorded.

Here, we assign the ^{1}H NMR peaks by making the deviation between the calculated and measured chemical shifts small and systematic. The calculated ^{1}H NMR chemical shifts of the

inner and outer pyrrole hydrogens are 8.24 and 12.33 ppm, respectively, as compared to the experimental values of 8.83 and 12.85 ppm reported in the supporting information of ref. 37. Comparisons of the calculated and measured ^{1}H NMR chemical shifts suggest that the lowest tautomer 2–4 was obtained in the synthesis, as the discrepancies between calculated and measured chemical shifts are less systematic when assuming that tautomers 1–4 or 3–4 have been synthesized. The tautomers with both pyrrole hydrogens inside the macroring can be ruled out, because they are strongly antiaromatic with ^{1}H NMR chemical shifts of 30–40 ppm for the pyrrole hydrogens. The ^{1}H NMR signals from the meso hydrogens should also appear in the vicinity but on both sides of 0 ppm in the experimental ^{1}H NMR spectrum. The calculated ^{1}H NMR chemical shifts of the studied tautomers are gathered in Table 2.

The three broad ^{1}H NMR signals originating from pyrrole hydrogens must be due to the presence of the nonaromatic 1–4, 2–4, and 3–4 tautomers in the sample, because the peaks appear in the range of 9–17 ppm in the experimental spectrum. Chang *et al.* did not report any details about the measurement of the experimental ^{1}H NMR spectrum with several N–H peaks.[37]

6 Magnetically induced currents

6.1 Aromatic character

The calculated current strengths and current pathways of the substituted porphyrinoids are shown in Fig. 1 and 2. The corresponding pictures of the nonsubstituted porphyrinoids are given in the ESI.† The strengths of the ring current around the porphyrinoid macroring of the substituted and nonsubstituted porphyrinoid tautomers are compared in Table 3.

Since the calculated ring-current strengths of the substituted porphyrinoid tautomers vanish or are negative *i.e.*, they are dominated by paratropic ring currents, they can be divided into two classes, namely nonaromatic and antiaromatic porphyrinoids, respectively. Calculations on the substituted porphyrinoids with and without the ethyl-formate group show that the substitution of the ethyl formate to the pyrrole ring B of the thienopyrrole moiety leads to a significant reduction in the antiaromatic character. The ethyl-formate substituent weakens the ring-current strength

This journal is © the Owner Societies 2014

Phys. Chem. Chem. Phys., 2014, **16**, 11010–11016 | **11013**

Table 3 Comparison of the calculated ring-current strengths (in nA T^{-1}) for the porphyrin macroring of the six tautomers of the substituted and nonsubstituted thienopyrrole-modified porphyrinoids. The changes in the ring-current strengths due to the substitution are also reported

Tautomer	Substituted	Nonsubstituted	Difference
1–2	−32.2	−46.0	13.8
1–3	−34.3	−50.0	15.7
2–3	−43.9	−56.1	12.2
1–4	−0.8	−14.2	13.4
2–4	−0.4	−11.7	11.3
3–4	−0.3	−11.5	11.2

around the porphyrinoid macroring by about 10 nA T^{-1}, whereas the effect from the methyl and ethyl groups in the β positions of the three ordinary pyrrole rings is about 2 nA T^{-1}. The alkyl substituted 2–4 tautomer without the ethyl-formate group is antiaromatic sustaining a paratropic ring current of −9.9 nA T^{-1} around the porphyrinoid macrocycle. Thus, the weaker paratropic ring current of the substituted porphyrinoids and the almost constant difference in current strengths of 11.2–15.7 nA T^{-1} between the substituted and nonsubstituted porphyrinoids are mainly due to the ethyl-formate substituent at ring B. The alkyl substituents in the β positions have a much lesser effect on the ring-current strength. The current strengths and the current pathways of tautomer 2–4 without the ethyl-formate group are given in the ESI.† Even though the reduction in the current strength changes the aromatic character, the weaker current strengths are not expected to significantly affect the relative energies because the ethyl-formate group diminishes the current strength by about the same amount for all tautomers. The current-density calculations also show that the net current strengths of 0.1–0.4 nA T^{-1} across the hydrogen bond is very weak.

The calculated aromatic character of the substituted porphyrinoid tautomers agrees qualitatively with the results obtained in the study by Chang et al.[37] However, they did not elucidate how the substituents affect the aromatic character of the thienopyrrole-modified porphyrinoids.

The nonsubstituted porphyrinoids are all antiaromatic sustaining paratropic ring currents around the macroring. However, the calculated ring-current strengths around the macroring show that the six nonsubstituted heteroporphyrin tautomers can also be grouped in two classes. The nonsubstituted porphyrinoids with only one inner hydrogen sustain weaker paratropic ring currents of −(11.5–14.2) nA T^{-1} as compared to paratropic current strengths of −(46.0–56.1) for the three other tautomers. Thus, tautomers 1–4, 2–4, and 3–4 with a hydrogen at the outer pyrrole nitrogen are less antiaromatic than tautomers 1–2, 1–3, and 2–3, which have both pyrrole hydrogens inside the macroring.

6.2 Current pathways

The GIMIC calculations provide detailed information about the current flow in multiring molecules. The current pathways in the molecules are obtained by calculating the current strengths passing through the chemical bonds. The detailed current pathways of the six tautomers of the substituted porphyrinoid

are shown in Fig. 1 and 2. The corresponding graphs for the nonsubstituted molecules and for the 2–4 tautomer of the alkyl substituted porphyrinoid without the ethyl-formate substituent are given in the ESI.† For the tautomers with two inner pyrrole hydrogens, the current pathways of the substituted and nonsubstituted porphyrinoids are similar. The main difference is the weaker paratropic currents in the substituted ones. For the tautomers with one pyrrole hydrogen at the outer nitrogen, the current pathways are qualitatively different as the substituted porphyrinoids are nonaromatic. In the following we discuss the current pathways of the individual tautomers.

1–2. Ring B sustains a diatropic current of 16.3 nA T^{-1}. The current pathway is split into inner and outer routes at the thiophene ring. The paratropic current is −20.2 nA T^{-1} along the inner pathway whereas a paratropic current of −12.3 nA T^{-1} takes the outer route. At ring D, the inner pathway dominates with a paratropic current of −25.8 nA T^{-1} as compared to −6.3 nA T^{-1} via the β carbons. The ring current of the macroring is split into the outer and inner pathways with paratropic currents of almost equal strengths at ring E. At ring A, the strength of the current along the inner route is −20.0 nA T^{-1} and the current strength along the outer route is −12.2 nA T^{-1}.

1–3. For rings A, B, and C, the current strengths are very similar to the ones of the same rings of tautomer 1–2. The current strengths and pathways of rings A and D of tautomer 1–3 are similar, whereas the inner route of ring E has a strong current of −26.4 nA T^{-1} as compared to −7.9 nA T^{-1} along the outer route.

2–3. Ring B sustains a very strong diatropic current of 24.0 nA T^{-1}. The paratropic ring current around the porphyrinoid macroring is split into two routes at the thiophene ring. The current along the inner pathway is −30.0 nA T^{-1} and the current along the outer route is −15.4 nA T^{-1}. The current is split into inner and outer pathways at rings D and E. The current strengths along the two branches are almost of the same size. The inner pathway dominates at ring A, whereas only −5.4 nA T^{-1} chooses the outer pathway.

1–4. The porphyrinoid macroring is nonaromatic with a very weak paratropic ring current of −0.8 nA T^{-1}. The pyrrole ring B is aromatic sustaining a diatropic current of 4.9 nA T^{-1}, which is smaller compared to the tautomers with two inner hydrogens. A diatropic current of 6.0 nA T^{-1} flows around the thiophene ring of the thienopyrrole moiety and continues around the pyrrole ring B. Thus, the pyrrole of the thienopyrrole moiety is aromatic, with a stronger diatropic current passing the pyrrole ring than passing the thiophene. The pyrrole rings of the porphyrinoid macroring are practically nonaromatic sustaining diatropic ring currents of 0.3–2.1 nA T^{-1} of which the pyrrole ring with the inner hydrogen sustains the strongest ring current.

2–4. The current pathways and current strengths of tautomer 2–4 are very similar to the ones obtained for 1–4. The diatropic ring current of the thienopyrrole rings is slightly stronger than that of tautomer 1–4.

3–4. The current pattern and strength of tautomer 3–4 are practically the same as for tautomer 2–4.

The calculations on the 2–4 tautomer of the thienopyrrole-modified porphyrinoid with and without the ethyl-formate

substituent at ring B show that the ethyl formate increases the current strength of the thiophene ring, whereas the current strength around ring B is practically unaffected by the presence of the ethyl-formate substituent. The weaker ring current around the thiophene part of the thienopyrrole renders the paratropic current flow around the porphyrinoid macroring feasible.

The common current pattern for the three antiaromatic tautomers is that the main share of the paratropic porphyrinoid ring current prefers the inner pathway at the pyrrole rings. The inner pyrrole hydrogen increases the resistance along the inner pathway leading to a division of the current flow into two branches of almost equal strengths. The pyrrole ring B is aromatic, whereas the thiophene ring is part of the porphyrinoid macroring in the same way as the three other ordinary pyrrole rings.

For the three nonaromatic porphyrinoids, the thienopyrrole moiety sustains a significant diatropic ring current of 6.0–9.7 nA T^{-1}. The diatropic ring current is stronger at the pyrrole ring than around the thiophene. The other pyrrole rings are practically nonaromatic sustaining weak diatropic and paratropic ring currents.

7 Conclusions

Magnetically induced currents as well as proton shieldings have been studied computationally for six possible N–H tautomers of a recently synthesized thienopyrrole-modified porphyrinoid. The calculated ring-current strength of the porphyrinoid macrocycle is practically zero for the tautomers with one inner hydrogen, whereas the three tautomers with two inner hydrogens are antiaromatic according to the ring-current criterion. The obtained aromatic characters of the lowest 2–4 tautomer are in qualitative agreement with the results recently obtained in the combined computational and experimental study by Chang et al.,[37] whereas we report in addition calculated ring-current strengths and pathways along the chemical bonds around the thiophene-modified porphyrinoid.

The current density calculations and the calculations of current strengths passing selected bonds yield the degree of aromaticity as well as the current and aromatic pathways of the tautomers. The pyrrole ring (B) of the thienopyrrole unit is aromatic for all tautomers. However, ring B sustains a stronger ring current for tautomers with a nonaromatic porphyrinoid macroring compared to the tautomers with an antiaromatic macroring. The thiophene ring fused to the pyrrole ring also sustains a diatropic ring current in the nonaromatic tautomers, whereas in the antiaromatic ones, the paratropic current around the porphyrinoid macrocycle splits into outer and inner branches at the thiophene ring. For the antiaromatic tautomers, the porphyrinoid ring current also splits into two branches at the three ordinary pyrrole rings. The ring current of the porphyrinoid ring prefers the inner pathway at the pyrrole rings. However, the inner hydrogen of the pyrrole rings increases the resistance along the inner pathway leading to a division of the current flow into two branches of almost equal strengths. The current density calculations also show that the presence of the ethyl-formate group at ring B stops the current flow around the porphyrinoid macroring for tautomer 2–4.

References

1 A. Osuka and S. Saito, Chem. Commun., 2011, 47, 4330–4339.
2 T. Higashino, J. M. Lim, T. Miura, S. Saito, J.-Y. Shin, D. Kim and A. Osuka, Angew. Chem., Int. Ed., 2010, 49, 1–6.
3 J.-Y. Shin, K. S. Kim, M.-C. Yoon, J. M. Lim, Z. S. Yoon, A. Osuka and D. Kim, Chem. Soc. Rev., 2010, 39, 2751–2767.
4 Z. S. Yoon, A. Osuka and D. Kim, Nat. Chem., 2009, 1, 113–122.
5 J. Sankar, S. Mori, S. Saito, H. Rath, M. Suzuki, Y. Inokuma, H. Shinokubo, K. S. Kim, Z. S. Yoon, J. Y. Shin, J. M. Lim, Y. Matsuzaki, O. Matsushita, A. Muranaka, N. Kobayashi, D. Kim and A. Osuka, J. Am. Chem. Soc., 2008, 130, 13568–13579.
6 T. K. Ahn, J. H. Kwon, D. Y. Kim, D. W. Cho, D. H. Jeong, S. K. Kim, M. Suzuki, S. Shimizu, A. Osuka and D. Kim, J. Am. Chem. Soc., 2005, 127, 12856–12861.
7 S. Saito, J. Y. Shin, J. M. Lim, K. S. Kim, D. Kim and A. Osuka, Angew. Chem., Int. Ed., 2008, 47, 9657–9660.
8 Y. Tanaka, S. Saito, S. Mori, N. Aratani, H. Shinokubo, N. Shibata, Y. Higuchi, Z. S. Yoon, K. S. Kim, S. B. Noh, J. K. Park, D. Kim and A. Osuka, Angew. Chem., Int. Ed., 2008, 47, 681–684.
9 J.-Y. Shin, K. S. Kim, M.-C. Yoon, J. M. Lim, Z. S. Yoon, A. Osuka and D. Kim, Chem. Soc. Rev., 2010, 39, 2751–2767.
10 H. Fliegl, D. Sundholm, S. Taubert and F. Pichierri, J. Phys. Chem. A, 2010, 114, 7153–7161.
11 H. Fliegl, D. Sundholm and F. Pichierri, Phys. Chem. Chem. Phys., 2011, 13, 20659–20665.
12 H. S. Rzepa, Org. Lett., 2008, 10, 949–952.
13 C. S. M. Allan and H. S. Rzepa, J. Org. Chem., 2008, 73, 6615–6622.
14 E. Steiner and P. W. Fowler, Org. Biomol. Chem., 2006, 4, 2473–2476.
15 E. Steiner and P. W. Fowler, Org. Biomol. Chem., 2004, 2, 34–37.
16 J. Aihara, Y. Nakagami, R. Sekine and M. Makino, J. Phys. Chem. A, 2012, 116, 11718–11730.

This journal is © the Owner Societies 2014

Phys. Chem. Chem. Phys., 2014, 16, 11010–11016 | 11015

17 J. Jusélius, D. Sundholm and J. Gauss, *J. Chem. Phys.*, 2004, **121**, 3952–3963.

18 H. Fliegl, S. Taubert, O. Lehtonen and D. Sundholm, *Phys. Chem. Chem. Phys.*, 2011, **13**, 20500–20518.

19 H. Fliegl and D. Sundholm, *J. Org. Chem.*, 2012, **77**, 3408–3414.

20 H. Fliegl, N. Özcan, R. Mera-Adasme, F. Pichierri, J. Jusélius and D. Sundholm, *Mol. Phys.*, 2013, **111**, 1364–1372.

21 R. R. Valiev, H. Fliegl and D. Sundholm, *J. Phys. Chem. A*, 2013, **117**, 9062–9068.

22 S. Taubert, D. Sundholm and J. Jusélius, *J. Chem. Phys.*, 2011, **134**, 054123.

23 H. Fliegl, D. Sundholm, S. Taubert, J. Jusélius and W. Klopper, *J. Phys. Chem. A*, 2009, **113**, 8668–8676.

24 E. Vogel, W. Haas, B. Knipp, J. Lex and H. Schmickler, *Angew. Chem., Int. Ed.*, 1988, **27**, 406–409.

25 E. Vogel, *J. Heterocycl. Chem.*, 1996, **33**, 1461–1487.

26 T. D. Lash and S. T. Chaney, *Chem. – Eur. J.*, 1996, **2**, 944–948.

27 T. D. Lash, J. L. Romanic, J. Hayes and J. D. Spence, *Chem. Commun.*, 1999, 819–820.

28 E. Steiner and P. W. Fowler, *ChemPhysChem*, 2002, **3**, 114–116.

29 M. K. Cyrañski, T. M. Krygowski, M. Wisiorowski, N. J. R. van Eikema Hommes and P. von Ragué Schleyer, *Angew. Chem., Int. Ed.*, 1998, **37**, 177–180.

30 J. I. Wu, I. Fernández and P. von Ragué Schleyer, *J. Am. Chem. Soc.*, 2013, **135**, 315–321.

31 J. Jusélius and D. Sundholm, *Phys. Chem. Chem. Phys.*, 1999, **1**, 3429–3435.

32 J. Jusélius and D. Sundholm, *Phys. Chem. Chem. Phys.*, 2000, **2**, 2145–2151.

33 J. Jusélius and D. Sundholm, *J. Org. Chem.*, 2000, **65**, 5233–5237.

34 P. von Ragué Schleyer, C. Maerker, A. Dransfeld, H. Jiao and N. J. R. van Eikema Hommes, *J. Am. Chem. Soc.*, 1996, **118**, 6317–6318.

35 R. Herges and D. Geuenich, *J. Phys. Chem. B*, 2001, **105**, 3214–3220.

36 D. Geuenich, K. Hess, F. Kohler and R. Herges, *Chem. Rev.*, 2005, **105**, 3758–3772.

37 Y. Chang, H. Chen, Z. Zhou, Y. Zhang, C. Schütt, R. Herges and Z. Shen, *Angew. Chem., Int. Ed.*, 2012, **51**, 12801–12805.

38 A. D. Becke, *J. Chem. Phys.*, 1993, **98**, 5648–5652.

39 C. Lee, W. Yang and R. G. Parr, *Phys. Rev. B: Condens. Matter Mater. Phys.*, 1988, **37**, 785–789.

40 F. Weigend and R. Ahlrichs, *Phys. Chem. Chem. Phys.*, 2005, **7**, 3297–3305.

41 M. Kollwitz and J. Gauss, *Chem. Phys. Lett.*, 1996, **260**, 639–646.

42 M. Kollwitz, M. Häser and J. Gauss, *J. Chem. Phys.*, 1998, **108**, 8295–8301.

43 A. M. Teale, O. B. Lutnæs, T. Helgaker, D. J. Tozer and J. Gauss, *J. Chem. Phys.*, 2013, **138**, 024111.

44 A. Klamt and G. Schüürmann, *J. Chem. Soc., Perkin Trans. 2*, 1993, 799–805.

45 R. Ahlrichs, M. Bär, M. Häser, H. Horn and C. Kölmel, *Chem. Phys. Lett.*, 1989, **162**, 165–169.

46 F. London, *J. Phys. Radium*, 1937, **8**, 397–409.

47 H. F. Hameka, *Mol. Phys.*, 1958, **1**, 203–215.

48 R. Ditchfield, *Mol. Phys.*, 1974, **27**, 789–807.

49 K. Wolinski, J. F. Hinton and P. Pulay, *J. Am. Chem. Soc.*, 1990, **112**, 8251–8260.

50 JMOL: an open-source Java viewer for chemical structures in 3D., http://www.jmol.org.

51 GIMP: GNU Image Manipulation Program, http://www.gimp.org.

52 H. Fliegl, O. Lehtonen, D. Sundholm and V. R. I. Kaila, *Phys. Chem. Chem. Phys.*, 2011, **13**, 434–437.